Journal of Applied Physics

Drying of salt contaminated porous media: Effect of primary and secondary nucleation

Cite as: J. Appl. Phys. **118**, 114901 (2015); https://doi.org/10.1063/1.4930292
Submitted: 09 May 2015 • Accepted: 27 August 2015 • Published Online: 15 September 2015

Julie Desarnaud, Hannelore Derluyn, Luisa Molari, et al.

Drying of salt contaminated porous media: Effect of primary and secondary nucleation

Julie Desarnaud,[1] Hannelore Derluyn,[2] Luisa Molari,[3] Stefano de Miranda,[3] Veerle Cnudde,[2] and Noushine Shahidzadeh[1,a)]
[1]*Van der Waals-Zeeman Institute, Institute of Physics, University of Amsterdam, Science Park 904, 1098 XH Amsterdam, The Netherlands*
[2]*Department of Geology and Soil Science – UGCT, Ghent University, Krijgslaan 281 S8, 9000 Gent, Belgium*
[3]*DICAM, Alma Mater Studiorum, University of Bologna, Viale Risorgimento 2, 40136 Bologna, Italy*

(Received 9 May 2015; accepted 27 August 2015; published online 15 September 2015)

The drying of porous media is of major importance for civil engineering, geophysics, petrophysics, and the conservation of stone artworks and buildings. More often than not, stones contain salts that can be mobilized by water (e.g., rain) and crystallize during drying. The drying speed is strongly influenced by the crystallization of the salts, but its dynamics remains incompletely understood. Here, we report that the mechanisms of salt precipitation, specifically the primary or secondary nucleation, and the crystal growth are the key factors that determine the drying behaviour of salt contaminated porous materials and the physical weathering generated by salt crystallization. When the same amount of water is used to dissolve the salt present in a stone, depending on whether this is done by a rapid saturation with liquid water or by a slow saturation using water vapor, different evaporation kinetics and salt weathering due to different crystallization pathways are observed. [http://dx.doi.org/10.1063/1.4930292]

INTRODUCTION

The presence of mineral salt crystals in porous media greatly affects the behavior of such materials. In civil engineering and geology, salt crystallization (also referred as haloclasty) is one of the major causes of mechanical or physical weathering causing disintegration of rocks and building materials.[1–6] On the other hand, the crystallization of salts in soil causes salinisation and sodification, which are amongst the most important forms of soil degradation causing desertification and threatening to the ecosystems.[6,7] The increase in impermeability of deep soil layers and rocks due to salt crystallization causes problems for oil well productivity and CO_2 sequestration.[8,9]

There can be various origin of salts present in porous media; the salts can be derived from external sources (e.g., capillary rising ground water, eolian origin, sea water along rocky coasts, or atmospheric pollution) or can be naturally present in the materials used for construction (such as mortars and bricks). With the variation in climatic conditions such as the temperature or relative humidity (RH), or rain followed by drying, salts crystallize either in the form of efflorescence (at the surface) or subflorescence (within the pore network).[10,11] Subsequently, once crystallized, salts can redissolve in two different ways: by bringing it in contact with liquid water (dissolution) or by contact with water vapor (deliquescence). The latter is due to the hygroscopic properties of salts. The resulting salt solution is subsequently mobilized in the porous network and gets re-crystallized when dried again, e.g., due to relative humidity variations.

The reaction of salts on water evaporation and weathering of porous media has attracted a lot of attention over the past decade, but remains incompletely understood. Most of studies reported up till now in the literature deal either with unidirectional (1D) evaporation of a saturated porous media containing homogeneous salt solutions or with evaporation-wicking experiments. In the 1D experiments, the extreme surface is exposed to evaporation; in a typical evaporation-wicking experiment, the porous material is permanently supplied with the salt solution, leading to a steady-state evaporation.[11–16]

These studies have revealed the impact of the pore size[17,18] and the relative humidity[19] on the type of crystallization. Mainly efflorescence has been observed in different types: crusty or patchy[17,18] (also referred to as "cauliflowers"[20]), and although it has been observed that the crystallization affects the drying rate, there are still many aspects that need to be clarified in order to understand the interplay between salt crystallization and evaporation. One important aspect that has not been taken into account so far is the dynamics of the crystallization and recrystallization processes.[21–24] In general, recrystallization that results from cycling differs from crystallization because in direct crystallization the crystallization is rapid, and with the resulting phase transition, solid contains many trapped impurities.[25] In addition, depending on whether the nucleation is primary (directly from solution) or secondary (from pre-existing crystallites present in the solution), different growth rates and crystallization patterns can result.[22,26–31] In primary nucleation, high supersaturations can be achieved. This is, for example, the case for the evaporation of homogeneous salt solutions in confined systems.[29,30] On the other hand, secondary nucleation typically happens around the saturation concentration.[24,25] It is clear from the above that the

a)Author to whom correspondence should be addressed. Electronic mail: n.shahidzadeh@uva.nl

crystallization dynamics in a porous medium depends on both thermodynamic and transport processes. These will also have a direct impact on the evaporation rate of the solvent (water) from the porous network.

In this paper, we show that the mechanisms of nucleation (primary or secondary) and crystal growth are of major importance for understanding the drying behavior of salt contaminated materials.

Porous materials that contain salts can be permanently exposed to dissolution/deliquescence-drying cycles, and we report that the dynamics of crystal growth is of paramount importance on both the evaporation rate and the possible damage generated by the salt crystallization. When the same amount of water is used to dissolve the salt present in a stone, different recrystallization patterns and evaporation kinetics can be found if this is done in different ways: by a rapid saturation with liquid water or by a slow saturation using water vapor.

EXPERIMENTAL

We perform a multiscale study on the behavior of sodium chloride contaminated sandstones, exposed to different RH conditions, roughly representative of winter and summer conditions. We have chosen sodium chloride because its solubility is only weakly temperature dependent, so that the main driving forces for (re-)crystallization are RH variations. Solutions were prepared with Sigma Aldrich grade 99.9% NaCl and Ultrapure Millipore water.

Macroscale experiments consist of studying the crystallization pattern and the drying kinetics of saturated sandstones (porosity $\sim 29\%$, and pore diameter $d_p \sim 30\,\mu$m). We study the recrystallization behavior and the drying of the salt-contaminated sandstones once they were rewetted with liquid water or brought in contact with water vapor ($RH \sim 100\%$). The global drying kinetics (evaporation in three-dimensional (3D) directions) are followed on an automated balance with a precision of 0.001 g placed in a homemade, controlled climatic chamber at $T = 21\,^{\circ}C$, and $RH \sim 20\%$ and 50%.[28] The dissolution/deliquescence followed by recrystallization cycling are repeated up to 5 times for each sample. To investigate whether there is an impact of sample size on the results, all experiments are repeated using three different sizes of sandstones: small (4×8 mm, with a volume to evaporative surface ratio of $V/S = 0.8$ mm), medium (8.5×8.5 mm, $V/S = 1.7$ mm), and large (20×40 mm, $V/S = 4.4$ mm).

Microscale experiments are used to investigate the crystallization in the core of the stone and at the surface in more detail. These experiments are done using high resolution X-ray computed tomography (μ-CT), optical and Scanning Electron Microscopy (SEM) combined with Energy-Dispersive X-ray (EDX).

X-ray μ-CT was performed at the Centre for X-ray Tomography at the Ghent University (UGCT) using the scanner HECTOR.[32] The resulting voxel size of the reconstructed datasets was $5\,\mu m^3$. The samples were initially scanned after the salt crystallization cycles, and subsequently washed out to be scanned in their natural state. The 3D reconstructions of the scans were done using the software Octopus.[33] Afterwards, the two datasets of each sample, i.e., after salt crystallization and after being washed out, were loaded in the software DataViewer (SkyScan). The datasets were roughly aligned manually and subsequently an automatic registration procedure was performed to optimize the 3D alignment in order to obtain the same positioning in 3D space for both datasets. This allows to assess changes in the sample, by subtracting the volume of the natural state from the volume of the salt-containing sample. At locations where salt crystals have precipitated, a change of the gray value is expected in the X-ray images. The differential volume obtained from the digital image subtraction thus represents the salt precipitation in the sample. 3D renderings of the samples and the precipitated salt were made in VG Studio Max.

It should be noted that this method is limited by the spatial resolution of the micro-tomographic datasets, i.e., 5 μm in this study. However, image analysis proved that we captured almost the full pore space with this resolution[32,33] (27.1% porosity based on image analysis; 28% porosity based on mercury intrusion porosimetry $\sim 30\,\mu$m average pore size of the uni-modal pore system).[6,34]

In addition, we use square microcapillaries as simple model systems for a single pore within a porous medium, to investigate the kinetics of dissolution and deliquescence of crystals, followed by recrystallization.[31] Quantifying small-scale features is fundamental to improving our understanding of the underlying basis of macroscopic fluid and solute transport behavior.

RESULTS

During a first series of experiments, the sandstones samples are saturated by imbibition with NaCl solutions (at saturation: 6.1 M). Figure 1 shows the drying at the two relative humidities for the different sample sizes. At RH $\sim$50%, the typical drying behavior is a constant drying rate period (CRP) followed by a much slower drying that sets in at a very late stage, almost at complete desaturation (Fig. 1-right). Comparing to pure water, the drying rate of the salt solution is lower. This is expected since the water activity is reduced in the presence of dissolved salt: the equilibrium vapor pressure above a saturated brine solution 1.88 kPa is significantly below that of pure water: 2.49 kPa.[35] The CRP is clearly associated with a homogeneous desaturation of the sample due to capillary flow at the surface.[36–38] This behavior does not depend on the size of the sample and shows that there is a continuous liquid film at the surface of the porous medium. The μ-CT and SEM analysis of the crystallization pattern at the end of drying show a heterogeneous distribution of salt crystals at the surface and a large amount of small cubic microcrystallites grown onto each other (also called patch[16,19] or "cauliflower structure"[20]) (Figs. 2 and 3–bottom). Hardly any salt crystal is detected in the core of the sample independently of its size. Such crystallization dynamics can be explained as follows: the surface is hydraulically connected to the core of the sample through the wetting films, taking care of the transport of the salt ions to the surface of the porous stone. The first crystallization then starts at the surface since the water evaporates there, and the

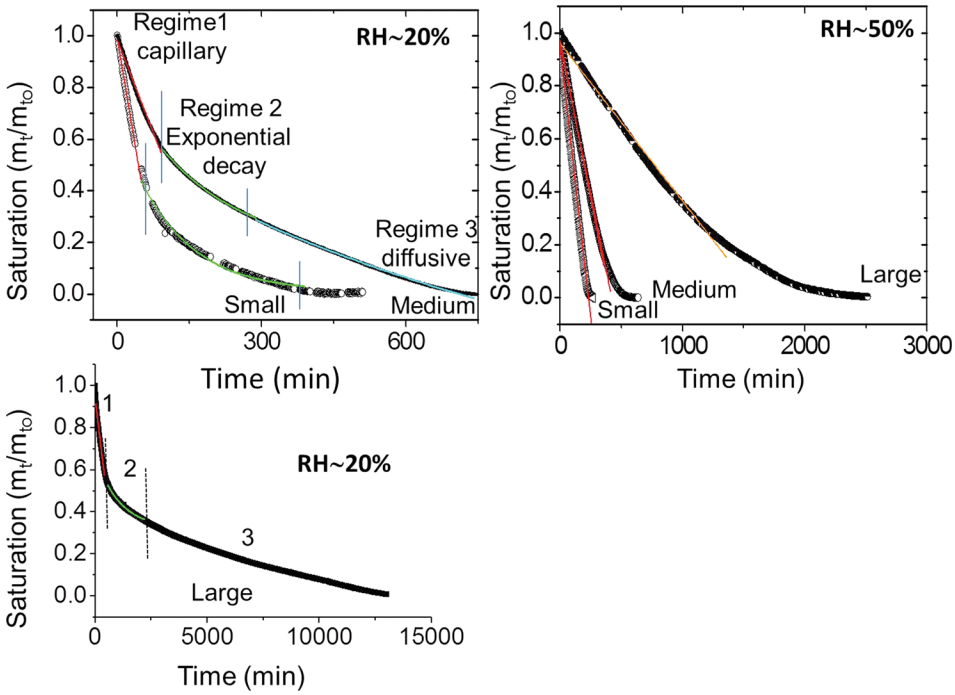

FIG. 1. Normalized water content at time t (m_t/m_{t0}) as a function of time (min) for different sample sizes (large, medium, and small) at two different relative humidities roughly representative of: Right: summer (RH ~50%): one CRP regime; left: winter (RH ~20%). Three regimes are observed: Medium sample: regime 1(CRP): $m_t/m_{t0} = -0.0049\,t + 0.986$; regime 2: $m_t/m_{t0} = 0.79\,e^{-0.003t}$; and regime3: $m_t/m_{t0} = -0.026\,t^{1/2} + 0.79$.

formation of the first crystal acts as a seed for further crystallization (secondary nucleation), leading eventually to the cauliflower structure (Figs. 2 and 3–bottom). In parallel, the precipitation process of several microcrystallites also induces a roughness of the surface that leads by capillary suction to an enhanced spreading of the fluid.[20,39] This leads to a creeping motion of the salt.[20,40,41]

At lower relative humidity (RH 20%), the drying behavior of the sample consists of three regimes: first, a CRP with a faster evaporation rate compared to RH 50%. The CRP

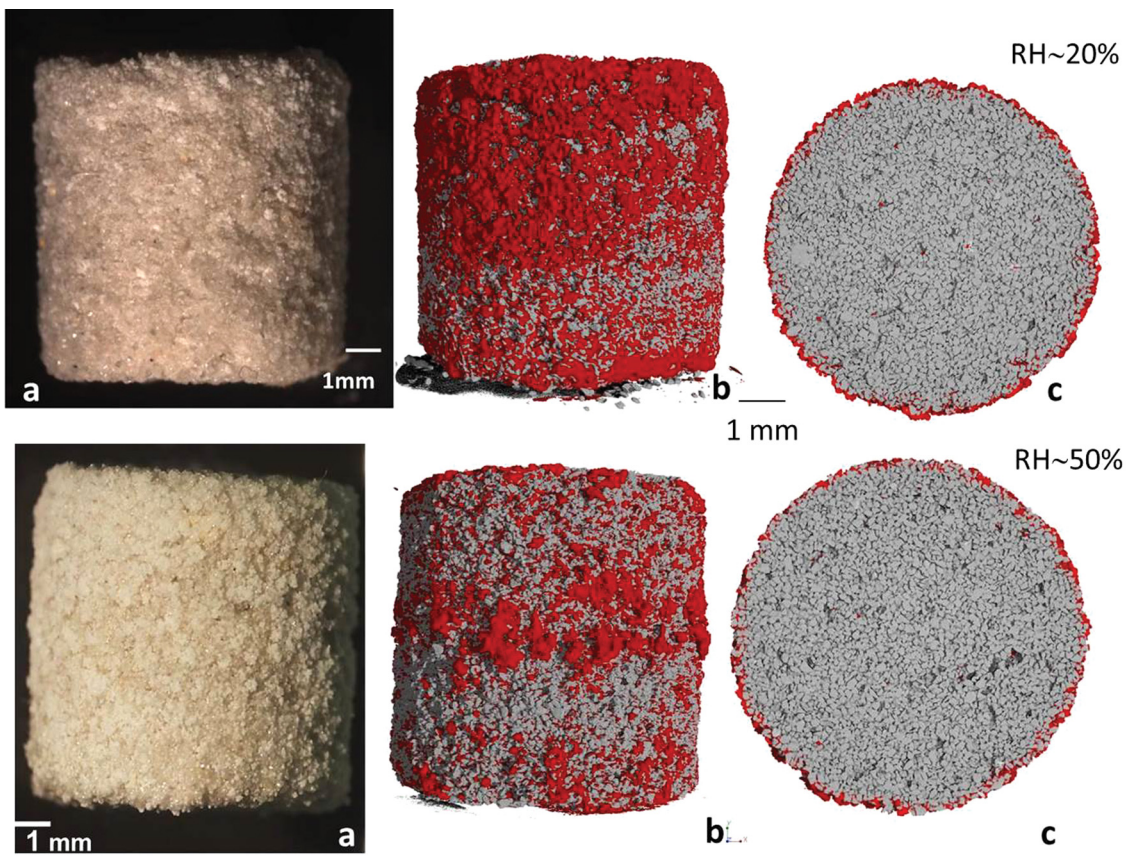

FIG. 2. Crystallization pattern after evaporation of saturated salt solution in sandstone: at RH 20% (top) and at RH 50% (bottom). (a) Image of the medium samples after drying. (b) and (c) X-ray μ-CT analysis of NaCl at the surface and in the core (middle level) of the samples.

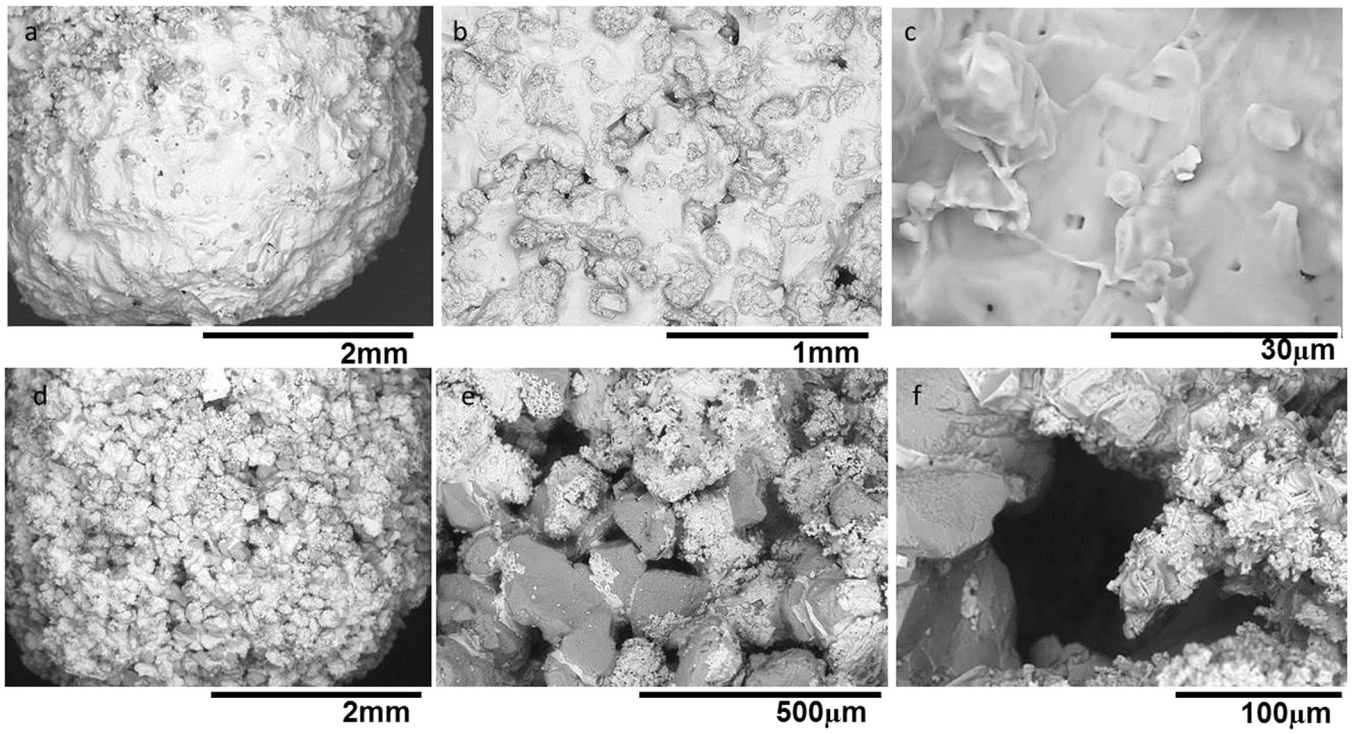

FIG. 3. SEM microphotographs of salt crystals at the surface of sandstone at the end of drying of sandstone saturated with salt solution. Top: drying at RH ~20%. (a) and (b) Formation of salt skin at the surface. (c) Porous structure of this crust layer. Bottom: drying at RH 50%. (d) Localised crystallization. (e) Crystallization between grains probably in the capillary liquid bridges. (f) Assemblies of several micro crystallites at the entrance of a pore (cauliflower structure).

regime is again independent of the sample size and continuous until the residual saturation is roughly half of the initial saturation. In the second regime, the saturation no longer decreases linearly in time, but much faster: the saturation follows an exponential decrease. The third regime is much slower: a $t^{1/2}$ dependence of the saturation as a function of time is found, characteristic of a mass transfer limited by diffusion that controls the evaporation (Fig. 1-left).[36,37]

This leaves the question what the origin is of the second (exponential decay) regime followed by a diffusive regime for drying at low relative humidity. Microscale analysis of the sample reveals the formation of salt crystals layer at the surface of the sample (Fig. 3), and no crystals are observed in the core of the sample (Fig. 2). The lateral rapid growth of salt crystals forms a skin on the outer surface of the sandstone, which forms a barrier and prevents the fluid from reaching the surface to evaporate. In fact, the skin formation accounts for the exponential decrease of the drying rate with time: with the growth of the skin layer, the evaporative surface rapidly becomes smaller in time, which slows down the evaporation. In fact, the drying rate is proportional to the surface of evaporation

$$\frac{dm}{dt} = -cA. \tag{1}$$

As soon as crystals start to grow at the surface, the evaporative surface decreases according to

$$\frac{dA}{dt} = \alpha \frac{dm}{dt}. \tag{2}$$

Consequently, the combination of these two differential equations for the evaporated mass gives

$$\frac{d^2m}{dt^2} = -c\alpha \frac{dm}{dt}, \tag{3}$$

which has an exponential solution: $m = m_0 e^{-c\alpha t}$, as is observed in the experiments.

A more detailed investigation of the crust shows that the salt layer (skin layer) that covers the outer surface of the sandstone is, in fact, also porous with a mean pore size of about 3 μm, i.e., 10 times smaller than the pore radius of sandstone (Fig. 3(c)). The average thickness of the salt skin is estimated from micro-CT results and SEM images. Both methods give a maximum thickness of the salt skin around 250 μm ± 50 μm. According to Washburn's law,[42] reducing the pore diameter will reduce the speed of fluid transport through capillary suction. Here, the speed of the capillary flow through these small pores is found to be insufficient to overcome the evaporation rate at low RH (20%). This leads to a rupture of the wetting films at the outer surface; subsequently, diffusive transport of vapor through the small pores controls the drying kinetics in the third regime. The diffusive transport in the third regime can consequently be well understood by taking into account theoretical models for the effect of the skin in the diffusion controlled evaporation[43,44] and the theoretical approach on the evaporation in a porous media in the presence of a drying front.[45] At the end of the regime 2, we consider that almost the whole surface of the stone is covered by a thin salt layer. Here, we assume that the salt skin and the stone are homogeneous with a boundary

between the two, which is well defined. We consider a gradient of concentration only along the x-axis due to a gradient of vapor pressure (i.e., relative humidity, $RH = \frac{P_w}{P_w^s} \times 100$) with p_w the vapor pressure and P_w^s the saturated water vapor pressure at 21 °C (2.487 kPa) (Fig. 4). At the top of the free surface of the salt skin, the vapor pressure is controlled by imposing a relative humidity of RH ~20% ($p_w^{20} = 0.497$ kPa). Under the salt skin, i.e., within the porous materials, the liquid salt solution is continuous throughout the sandstone. The vapor pressure just above this (i.e., at the boundary between the stone and the precipitated salt) is equal to the vapor pressure above the saturated NaCl solution, $p_w^{75} = 1.865$ kPa.

If the evaporation rate in the third regime is diffusion controlled, following Fick's law, the rate of transfer of diffusing water vapor through a unit area of a section of the thin salt skin is proportional to the concentration gradient normal to the section

$$J_w = \frac{1}{S}\frac{dm}{dt} = -D_{eff}\frac{dc_w}{dx}, \tag{4}$$

where D_{eff} is the effective diffusion coefficient in the porous skin and S is the free evaporative surface. Considering the ideal gas behavior of water vapor, we can write the relation between the vapor pressure and the water vapor concentration as

$$c_w = \frac{p_w M}{RT}, \tag{5}$$

where p_w is the vapor pressure, M is the molar mass, R is the gas constant, and T is the temperature of the gas. By substituting Equation (5) in Fick's law, we obtain

$$J_w = \frac{1}{S}\frac{dm}{dt} = -D_{eff}\frac{M}{RT}\frac{\left(p_w^{75} - p_w^{20}\right)}{l\,(t)}, \tag{6}$$

where l is the thickness of the skin and $\Delta p_w = p_w^{75} - p_w^{20}$ is the difference between the vapor pressure between the two sides of the surface skin. Considering the porous structure of the salt skin, the amount of precipitated salt which makes the skin can be written as

$$m_{NaCl} = \rho_{Nacl}.S.l.\,(1-\phi), \tag{7}$$

where ϕ is the porosity of the salt skin, ρ is the salt density, and S is the surface of the sample. Moreover, the amount of NaCl that precipitates is related to the amount of evaporated water by the relation: $m_{NaCl}(t) = 0.36\,.\,m_w(t)$.

By combining these two equations, we obtain the expression of the thickness of the skin as a function of the weight of evaporated water

$$l = \frac{0.36.m_w}{\rho_{Nacl}.S.(1-\phi)}. \tag{8}$$

By incorporating the expression of l in the evaporation flux equation and after integration, we obtain

$$\Delta m_w = -\left(\frac{2D_s M \Delta p_w \rho_{Nacl} S^2}{0.36RT}\right)^{1/2}.t^{1/2}. \tag{9}$$

Here, the Δm_w is the amount of evaporated water from the start of the 3rd regime and $D_s \sim D_{eff}(1-\phi)$ is the equivalent coefficient of diffusion in the porous skin. Depending on the simplifying assumptions and idealizations, various relations between the effective diffusion coefficients D_{eff} and porosity, ϕ, can be found in the literature.[46,47]

Comparing the prefactor of Eq. (9) to the experimental data (Fig. 4), we obtain $D_{s\sim} \sim 3 \times 10^{-5}$ cm^2/s, and the lower value of D_s compared to the diffusion coefficient of water vapor through air is ($D = 0.242$ cm^2/s) due to the effects of the porosity and tortuosity of the porous salt skin. The value that we obtain is on the same order of magnitude as that in a porous membrane with a pore diameter around ~2 μm and a porosity around 5%.[48] As was shown by different authors, the diffusion coefficients in porous media D_p can be significantly smaller than those in the bulk D_f. Moreover, as the fluid-filled porosity decreases, D_p/D_f also decreases owing to increased tortuosity and decreased cross section for diffusion.[44,48]

The duration of the diffusive regime increases with the size of the sample, as is expected: if the sample is very large (V/S ratio high), there will be a lot of liquid in the sample when the liquid film at the surface of the crust disappears, and consequently, the diffusive regime becomes very long. For the small samples (V/S = 0.8 mm) for which the end of the second regime coincides with a complete desaturation of the sample, the diffusive regime is then no longer observed (Fig. 1). Another interesting conclusion from these different observations is that for a given sample the total drying time is *longer* at low relative humidity (RH = 20%) compared to the high one (RH = 50%), due to the subtle interplay between crystallization dynamics and evaporation. This observation is in a good agreement with the results obtained for the 1D drying of NaCl saturated brick samples at RH ~0% and RH >55%.[19]

Recrystallization dynamics: After the initial drying described above, we bring the NaCl-contaminated sandstones

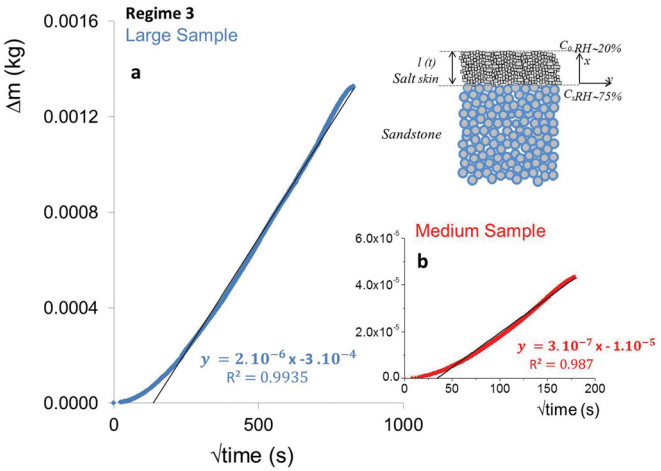

FIG. 4. Right: Scheme of the salt skin at the surface of the stone and the concentration gradient normal to the section. The evaporated mass of water in the third regime as a function of square root of time for (a) large and (b) medium samples dried at RH ~20%. The line shows the linear trend, i.e., the diffusion controlled evaporation process through the porous salt skin.

in contact either with liquid water (dissolution) or with water vapor ($RH > RH_{eqNaCl,}$ deliquescence) until complete saturation. Once saturated, the sample is dried again at 20% and 50% RH. We have repeated this cycling up to 5 times.

Dissolution-drying experiments: In the case of saturation by rewetting with pure water which is a rapid process, we observe that independently of the relative humidity, not all salt crystals at the surface will have time to dissolve and distribute again inside the stone before the evaporation starts. Subsequently, drying induces the secondary nucleation of new crystals on top of the existing, incompletely dissolved ones. In this situation, low supersaturations and small induction times are observed because the nucleation and growth take place on existing crystal surfaces once the evaporation starts. The rewetting is done with pure water, so no additional salt is added. The observed precipitation of the new crystals at the surface thus implies the dissolution of crystals within the sample and the transport of material to the place where the growth proceeds on the outer surface. Therefore, rewetting followed by drying cycles tends to extract (transport) the salt from within the porous medium towards the outer surface by forming large cauliflower-like salt crystal assemblies at the surface (Fig. 5(b)).

The increase in size of the cauliflowers with increasing number of wetting/drying cycles leads (Figs. 5 and 3(f)) consequently to the disappearance of the "skin" at the surface of the sample, which in the first cycle significantly reduced the evaporation rate for low relative humidity (RH $\sim$ 20%). This crystallization dynamics has its direct repercussions on the drying behaviour as it can be seen in Figure 6. First, with increasing the number of cycles, the drying kinetics gets closer to the drying kinetics of water. Second, the exponential regime associated with the formation of a salt "skin" that slowed down the evaporation disappears completely due to the fact that the skin layer disappears with cycling as discussed above. Third, because the skin layer is subsequently replaced by large cauliflowers with cycling, the constant rate period extends over a longer period with increasing the number of cycles. The drying dynamics can thus be described as a constant rate period due to the capillary transport to the surface followed by a diffusive regime. The transition between these two regimes becomes smaller and smaller with subsequent cycling. It is important to note that, contrary to what happened for the first cycle, after several rewetting/drying because the effect of the salt layer has disappeared, the evaporation at low RH then becomes faster than at high RH, as is expected intuitively (Fig. 6).

For high relative humidity RH $\sim$50% (lower evaporation rates), no skin formation was found in the first cycle, and the exponential regime was absent. Consequently, the drying behavior is not affected by the recrystallization dynamics as is borne out by the observation that subsequent cycles do not lead to different drying rates (Fig. 6).

DELIQUESCENCE-DRYING EXPERIMENTS

If the water is re-introduced into the porous medium by deliquescence, a very different recrystallization dynamics is observed. The experiments show that the formation of large cauliflowers of crystals due to secondary nucleation upon recrystallization is almost completely absent with the increase in the number of cycles. The deliquescence of the salt crystals is a slow process, which leads to the formation of a very homogeneous saturated salt solution, which

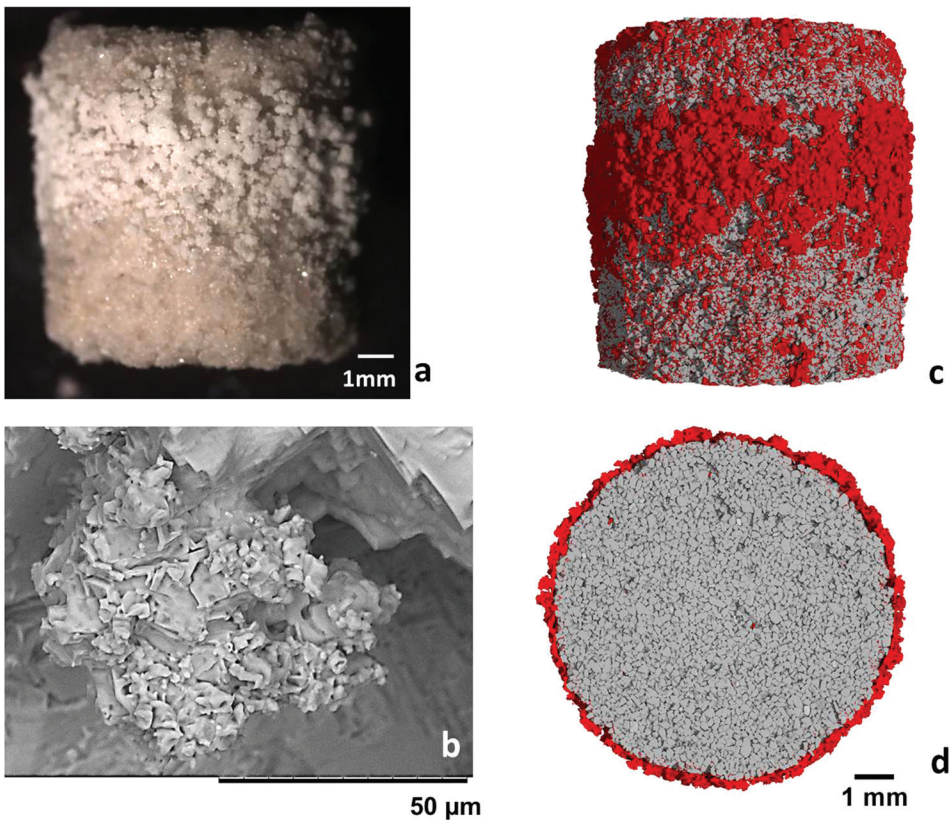

FIG. 5. Recrystallization due to 5 dissolution–drying cycles at RH $\sim$ 20%. (a) Localisation of the crystallization region with cycling; (b) SEM micrograph at the surface of the microcrystallites assemblies (cauliflower structures); (c) and (d) X-ray μ-CT analysis of NaCl at the surface and in the core (middle) of the sample.

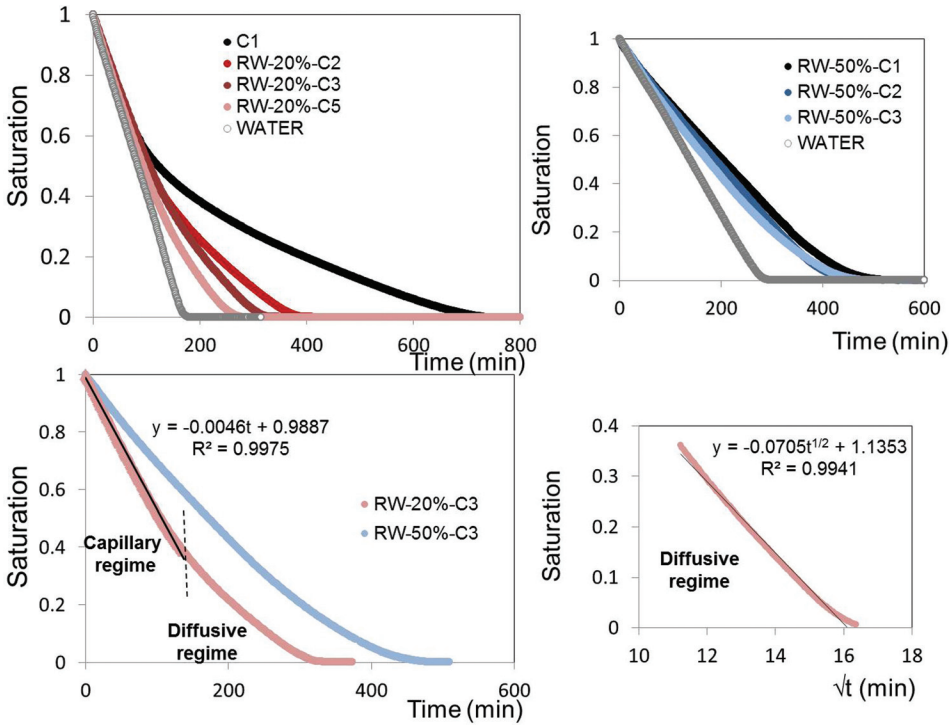

FIG. 6. Drying kinetics with several dissolution-drying cycles. (a) RH ∼20%; Grey curve: water; black curve: NaCl solution (6.1 M) cycle 1; Shades of red: 3 drying curves after wetting with water. (b) RH ∼50%, shades of blue: 2 drying curves after wetting with water. (c) Comparison of the drying curve after three cycles: pink curve at RH ∼20% and blue curve at RH ∼50%. (d) Diffusive regime at 20% relative humidity.

gradually invades the porous network of the stone, thus transporting the salt to the interior of the stone. The subsequent recrystallization (as a primary nucleation) of the homogeneous salt solution leads to the increase of the number of large cubic crystals (Fig. 7); their formation is usual for recrystallization because at each cycle impurities are expelled.[24,31]

It was recently shown that high supersaturations can be achieved during such recrystallization from homogeneous solutions of sodium chloride.[24,28,29] The increase of salt

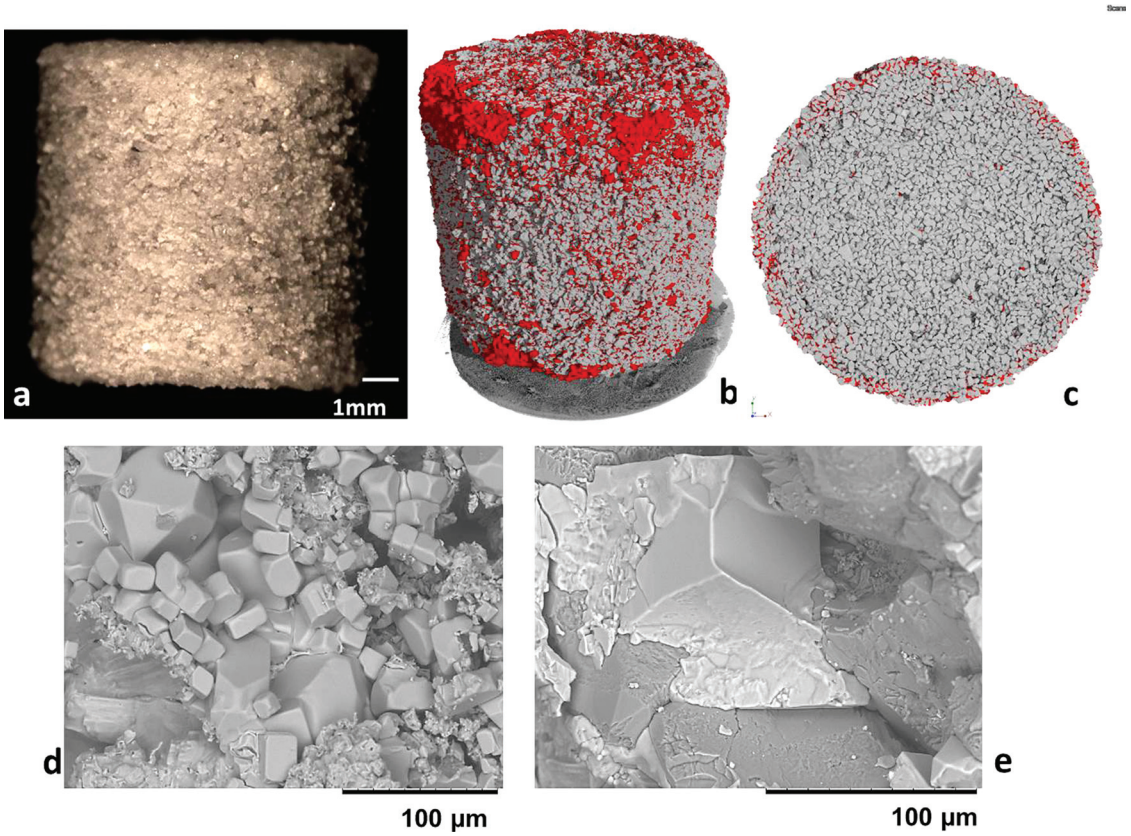

FIG. 7. Recrystallization due to several deliquescence–drying cycles at RH ∼20%. (a) and (b) Presence of less crystals at the surface. (c) X-ray μ-CT analysis: Migration of salt crystals (red) in the subsurface (subflorescence). (d) and (e) SEM pictures of large cubic crystals at the surface and between the grains at the subsurface after 3 cycles of deliquescence/drying.

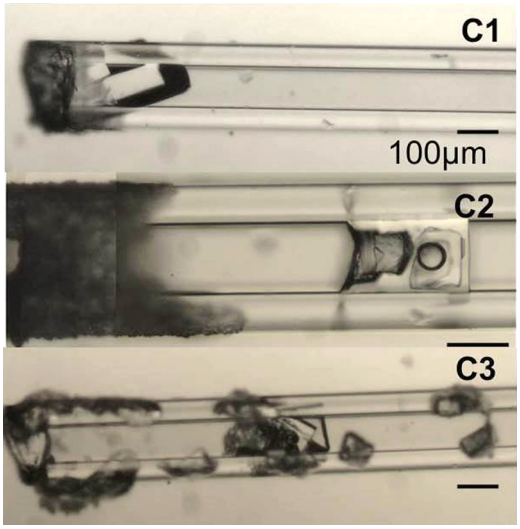

FIG. 8. 3 deliquescence-drying cycles in a 100 μm square microcapillary. By increasing the number of cycles, the blocking salt microcrystallites layer (skin) at the entrance disappears, and more cubic crystals are formed both at the outer surface and deeper inside the microcapillary.

concentration in the solution before recrystallization reduces the wetting properties of the solution. This leads to an increase of the surface tension and contact angle of the salt solution on glass slide, measured experimentally, as $\gamma_{lv} = 13.826\ (S) + 71.38$ and $\theta_{ls} = 20.11(S) + 30.41$ with $S = m_i/m_{0,}$ where m_0 represents the saturation concentration (6.1 mol. kg^{-1}) and m_i the NaCl concentration in the solution. This can be the cause of the retraction of the solution into the porous network and the crystallization in the subsurface, as it is clearly visible from microtomography images.

To confirm this hypothesis, we did some experiments in single square microcapillaries representative of a single pore in the porous network. The result confirms well that with increasing the number of cycles of deliquescence/drying, there is a retraction of the salt solution due to the increase of concentration and the change in the wetting properties of the salt solution. As can be seen in Figure 8, at the first cycle, crystallization occurs at the entrance of the capillary with the formation of a layer blocking the main entrance. With two deliquescence-drying cycles, first, the skin at the entrance is gradually replaced by well-shaped cubic crystals at the outer wall of the microcapillary and a second part of the salt solution retracts inside of the capillary, leading to crystallization deeper in the microcapillary.

The increase of the concentration before the primary nucleation growth also affects the drying rate since the equilibrium vapor pressure above the sample decreases,[29] which slows down the drying. This leads to a slowing down of the evaporation rate in what we previously called the regime 1 "constant rate period" (Fig. 9). This can be seen with the linear fit of this regime. Moreover, in this recrystallization dynamics, the formation of crystals layer as skin due to lateral secondary nucleation growth is avoided. Therefore, as it is expected intuitively the evaporation at low RH ~20% remains faster than at high RH ~50% (Fig. 9).

After 3 to 5 subsequent saturation/drying cycles, the percentage of damage is assessed by gently removing salt efflorescence, washing out the remaining salt, drying the stone, and weighing the stone.[49] The amount of damage is then given by the weight loss of the stone

$$\text{Damage} = (M_{initial}^{drystone} - M_{final}^{washedstone} / M_{initial}^{drystone}) \times 100\%. \quad (10)$$

The results clearly show that first with deliquescence/drying cycles the percentage of efflorescence decreases with the progression of the number of cycles from 20% to 5% after 3 cycles. Second, such humidity cycling can lead to damage: 6% loss of materials is observed in the form of sanding. The

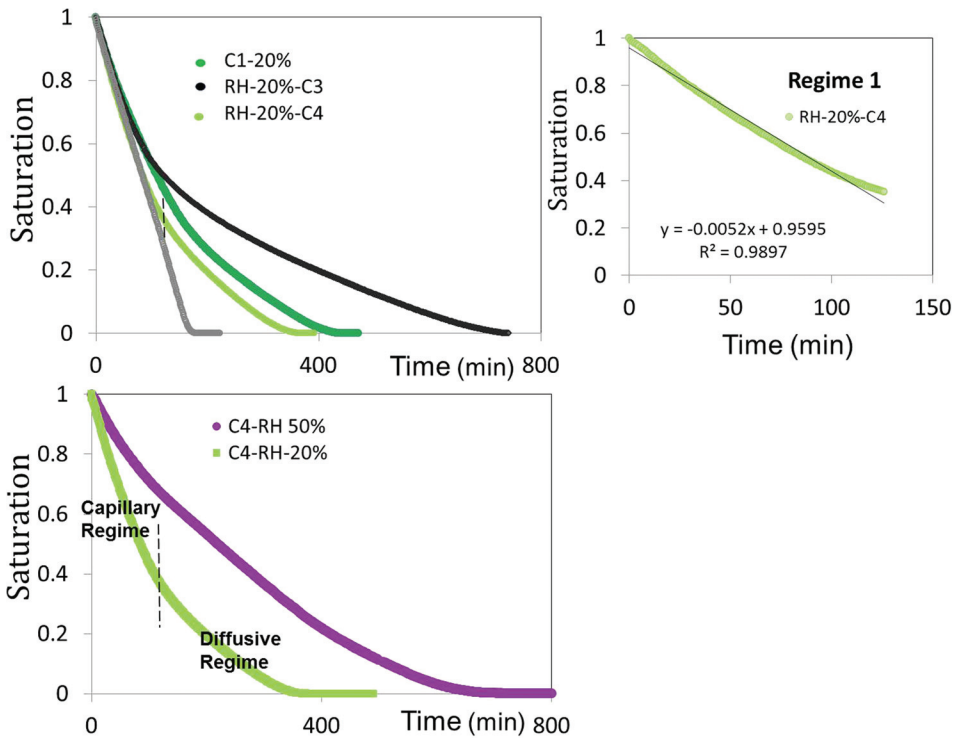

FIG. 9. Drying kinetics with several deliquescence-drying cycles on the same medium sample. (a) RH ~20%; Grey curve: pure water; black curve: Sodium chloride solution 6.1 M (cycle one); Shades of green: 2 drying curves after 2 complete deliquescence. The dotted line shows the direct transition between capillary and diffusive regime at RH 20%. (b) The behaviour of the capillary regime after 4 cycles and the linear fit. (c) Comparison of the fourth drying curves (C4) after three cycles of deliquescence at RH ~20% (green) and RH ~50% (violet). The diffusive regime: $y = -0.047\,t^{1/2} + 0.866$; and $R^2 = 0.996$.

faster growth of less nuclei with the progression of the cycles, which lead to larger cubic crystals in size at the subsurface, can also explain why repeated humidity cycling can lead to a gradual expansion of the material[50] causing more and more damage with the progression of cycles. To the contrary, hardly any damage is observed for the case of dissolution with liquid water, followed by recrystallisation (Fig. 10).

CONCLUSION

In this paper, we have investigated the effect of salt crystallization on the drying dynamics of salt-containing porous media, a subject of considerable importance in a variety of fields. We have elucidated the major role played by different salt crystallization pathways on the drying behavior of salt-containing sandstones subjected to several wetting-drying cycles. The kinetics of crystal growth, notably whether the nucleation is primary or secondary, strongly influences the drying behavior, and we provide a clear identification of the different possible regimes that are possible, depending also on external parameters such as the relative humidity and sample size. Three different regimes can be distinguished: (i) a capillary regime characterized by a constant evaporation rate; (ii) a *novel* regime in which the evaporation rate decreases exponentially due to the crystal growth that reduces the evaporative surface area, and (iii) a diffusive regime, in which the evaporative flux scales as $\sqrt{t}$; in this regime, the porous medium is almost completely covered with salt and the speed of the capillary flow through the small pores of the crust is insufficient to overcome the evaporation. We find that recrystallization due to subsequent cycling progressively decreases the surface coverage by the salt crust and hence the evaporation rate increases; after several cycles the intermediate regime associated with the formation of the salt crust disappears completely. The difference between dissolution by adding liquid water or deliquescence (by water vapor) is that liquid water progressively extracts the salt from the porous medium and forms a few large microcrystallites assemblies on its surface due to the secondary nucleation of crystals on incompletely dissolved crystals on the stone surface. Deliquescence is much slower and leads to complete dissolution. From the homogeneous salt solution that forms, we observe the crystallization of large cubic crystals that progress towards the *interior* of the stone core after several cycles. The results obtained here for NaCl are in good agreement with our previous work on sodium sulfate Na_2SO_4 for which humidity cycling and rewetting/drying also leads to different crystallization mechanisms due to the difference between the primary or secondary nucleation and the related supersaturation reached in the solution during drying.[28]

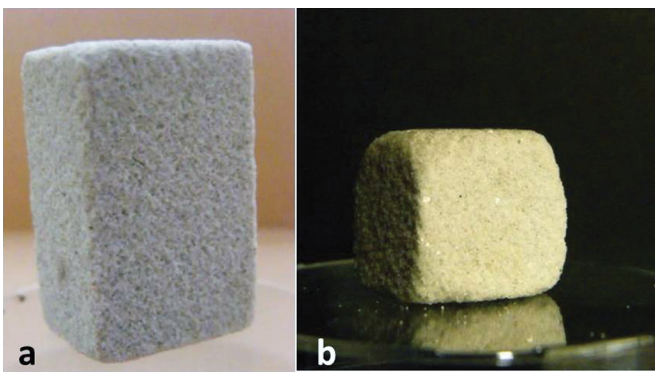

FIG. 10. Salt weathering due to 5 cycles of recrystallization in large sample (a) dissolution/drying: (a) damage <0.5% of the initial mass (b) deliquescence/drying; we observe sanding (granular disintegration) of the sample in the corners (damage ~6%).

These observations take all their importance if we consider salt weathering of stones, i.e., the damage to stones due to the crystallization of salts.[3] It has often been assumed that the crystals forming within the stone (subflorescence) or at its surface (efflorescence) is a property of the specific salt that is present;[3] here, we show that for the same salt, both phenomena can be observed depending on the experimental procedure. Efflorescence is often an aesthetic problem on buildings or wall paintings. Our results suggest that in any case for NaCl, this problem becomes worse if one tries to wash the salt off with liquid water but could be avoided by humidity cycling. Subflorescence, on the other hand, is believed to be the major cause of stone damage; the growing salt crystals exert a crystallization pressure onto the pore wall that may damage the stone.[4,5] Humidity cycling that may occur naturally (our RH values are typical of European summers and winters) is observed here to lead to the formation of larger and larger crystals. These typically form after several cycles and at high supersaturations,[28,29] and since the crystallization pressure is directly given by the supersaturation, this may lead to severe damage of sodium chloride contaminated sandstone.

ACKNOWLEDGMENTS

This work was part of the European Project KISADAMA, a JPI-Cultural Heritage: Joint Heritage European Programme. Hannelore Derluyn is a postdoctoral fellow of the Research Foundation—Flanders (FWO) and acknowledges its support.

[1]D. H. Everett, "The thermodynamics of frost damage to porous solids," Trans. Faraday Soc. **57**, 1541–1551 (1961).
[2]A. S. Goudies and H. A. Viles, *Salt Weathering Hazard* (Wiley, London, 1997).
[3]G. W. Scherer, "Stress from crystallization of salt," Cem. Concr. Res. **34**, 1613 (2004).
[4]M. Steiger, "Crystal growth in porous materials: I, the crystallization pressure of large crystals," J. Cryst. Growth **282**, 470 (2005).
[5]N. Shahidzadeh-Bonn, J. Desarnaud, F. Bertrand, X. Chateau, and D. Bonn, Phys. Rev. E **81**, 066110 (2010).
[6]V. N. Wong, R. C. Dalal, and R. S. Greene, "Salinity and sodicity effects on respiration and biomass of soil," Biol. Fertil. Soils **44**, 943–953 (2008).
[7]R. U. Cook and I. J. Smalley, "Salt weathering in deserts," Nature **220**, 1226–1227 (1968).
[8]N. Muller., R. Qi, E. Mackie, K. Pruess, and M. J. Blunt, "CO_2 injection impairment due to halite precipitation," Energy Proc. **1**, 3507–3514 (2009).
[9]Y. Peysson, "Permeability alteration induced by drying of brines in porous media," Eur. Phys. J.: Appl. Phys. **60**, 24206 (2012).
[10]C. Rodriguez-Navarro and E. Doehne, "Salt weathering: Influence of evaporation rate, supersaturation, and crystallization pattern," Earth Surf. Processes Landforms **24**, 191–209 (1999).

[11]H. P. Huinink, L. Pel, and M. A. J. Michels, "How ions distribute in a drying porous medium: A simple model," Phys. Fluids **14**, 1389–1395 (2002).
[12]L. Guglielmini, A. Gontcharov, J. Aldykiewicz, and H. A. Stone, "Intermediate time dynamics and efflorescence," Phys. Fluids **20**, 077101 (2008).
[13]S. Verran-Tissoires and M. Prat, "Discrete salt crystallization at the surface of a porous medium," Phys. Rev. Lett. **108**, 054502 (2012).
[14]N. Sghaier and M. Prat, "Effect of efflorescence formation on drying kinetics of porous media," Transp. Porous Media **80**, 441–454 (2009).
[15]H. Eloukabi, F. Sghaier, S. B. Nasrallah, and M. Prat, "Experimental study of the effect of sodium chloride on drying of porous media: The crusty-patchy efflorescence transition," Int. J. Heat Mass Transfer **56**, 80–93 (2013).
[16]N. Shokri, "Pore-scale dynamics of salt transport and distribution in drying porous media," Phys. Fluids **26**, 012106. (2014).
[17]F. Hidi, F. Sghaier, H. Eloukabi, M. Prat, and S. Ben Nasrallah, "Porous media coffee ring effect and others factors affecting the first crystallization time of the sodium chloride at the surface of a drying porous medium," Phys. Fluids **25**, 127101 (2013).
[18]S. Verran-Tissoires and M. Prat, "Evaporation of sodium chloride solution from a saturated porous medium with efflorescence formation," J. Fluid Mech. **749**, 701–749 (2014).
[19]S. Gupta, H. P. Huinink, M. Prat, L. Pel, and K. Kopinga, "Paradoxical drying of a fired-clay brick due to salt crystallization," Chem. Eng. Sci. **109**, 204–211 (2014).
[20]N. Shahidzadeh-Bonn, S. Rafai, D. Bonn, and G. Wegdam, "Salt crystallization during evaporation: Impact of interfacial properties," Langmuir **24**, 8599–8605 (2008).
[21]J. W. Mullin, *Crystallization*, 4th ed. (Butterworths-Heinemann, 2001.
[22]R. D. Doherty, D. A. Hughes, F. J. Humphreys, J. J. Jonas, D. J. Jensen, M. E. Kassner, W. E. King, T. R. McNelley, H. J. McQueen, and A. D. Rollett, Materials Science and Engineering A **238**, 219–274 (1997).
[23]D. W. Oxtoby, "Nucleation of first-order phase transitions," Acc. Chem. Res. **31**, 91–97 (1998).
[24]J. Desarnaud and N. Shahidzadeh-Bonn, "Salt crystal purification by deliquescence/crystallization cycling," Europhys. Lett. **95**, 48002 (2011).
[25]I. Sunagawa, "Growth and morphology of crystals," Forma **14**, 147–166 (1999).
[26]D. Aquilano, L. Pastero, M. Bruno, and M. Rubbo, "{100} and {111} forms of the NaCl crystals coexisting in growth from pure aqueous solution," J. Cryst. Growth **311**, 399–403 (2009).
[27]J. J. De Yoreo and P. Vekilov, "Principles of crystal nucleation and growth," Mineral. Soc. Am. **54**, 57–93 (2003).
[28]J. Desarnaud, F. Bertrand, and N. Shahidzadeh-Bonn, "Impact of the kinetics of salt crystallization on stone damage during rewetting/drying and humidity cycling," J. Appl. Mech. **80**, 020911 (2013).
[29]J. Desarnaud, H. Derluyn, J. Carmeliet, D. Bonn, and N. Shahidzadeh, "Metastability limit for the nucleation of NaCl crystals in confinement," J. Phys. Chem. Lett. **5**(5), 890–895 (2014).
[30]A. Naillon, P. Duru, M. Marcoux, and M. Prat, "Evaporation with sodium chloride crystallization in a capillary tube," J. Cryst. Growth **422**, 52–61 (2015).
[31]N. Shahidzadeh and J. Desarnaud, "Damage in porous media: Role the kinetics of salt (re)crystallization," Eur. Phys. J.: Appl. Phys. **60**, 24205 (2012).
[32]B. Masschaele, M. Dierick, D. Van Loo, M. N. Boone, L. Brabant, E. Pauwels, V. Cnudde, and L. Van Hoorebeke, "HECTOR: A 240 kV micro-CT setup optimized for research," J. Phys.: Conf. Ser. **463**, 012012 (2013).
[33]J. Vlassenbroeck, M. Dierick, B. Masschaele, V. Cnudde, L. Van Hoorebeke, and P. Jacobs, "Software tools for quantification of x-ray microtomography," Nucl. Instrum. Methods Phys. Res., Sect. A **580**, 442–445 (2007).
[34]Z. Pavlik, P. Michalek, M. Pavlikova, I. Kopecka, I. Maxova, and R. Cerny, "Water and salt transport and storage properties of Mšené sandstone," Constr. Build. Mater. **22**(8), 1736–1748 (2008).
[35]R. A. Robinson, "The vapour pressures of solutions of potassium chloride and sodium chloride," Trans. R. Soc. New Zealand **75**, 203–217 (1945).
[36]N. Shahidzadeh-Bonn, A. Azouni, and P. Coussot, "Effect of wetting properties on the kinetics of drying of porous media," J. Phys.: Condens. Matter **19**, 112101 (2007).
[37]M. Prat, "On the influence of pore shape, contact angle, and film flows on drying of capillary porous media," Int. J. Heat Mass Transfer **50**, 1455–1468 (2007).
[38]A. G. Yiotis, A. G. Boudouvis, and A. K. Stubos, "Effect of liquid films on the drying of porous media," AIChE J. **50**, 2721–2737 (2004).
[39]J. Bico, U. Thiele, and D. Quere, "Wetting of textured surfaces," Colloids Surf., A **206**, 41–46 (2002).
[40]R. Hirda and M. D. Bolton, "Upward migration of sodium chloride by crystallization on non-porous surfaces," Philos. Mag. **94**(1), 78–91 (2014).
[41]W. J. Enckevort and H. Los, "On the creeping of saturated salt solution," Cryst. Growth Des. **13**, 1838–1848 (2013).
[42]E. W. Washburn, "The dynamics of capillary flow," Phys. Rev. **17**, 273 (1921).
[43]J. Crank, *The Mathematics of Diffusion* (Claredon Press, Oxford, 1975).
[44]S. W. Webb and K. Pruess, "The use of Fick's law for modeling trace gas diffusion in porous media," Transp. Porous Media **51**, 327–341 (2003).
[45]P. Faure and P. Coussot, "Drying of model soil," Phys. Rev. E **82**, 036303 (2010).
[46]J. H. Kim, J. A. Ochoa, and S. Whitaker, "Diffusion in anisotropic porous media," Transp. Porous Media **2**, 327–356 (1987).
[47]D. Mu, Z. Liu, C. Huang, and N. Djilali, "Prediction of the effective diffusion coefficient in random porous media using the finite element method," J. Porous Mater. **14**, 49–54 (2007).
[48]H. Schmidt, D. Marcinkowska, and M. Cieslak, "Testing water vapour permeability through porous membrane," Fibers and Textiles in Eastern Europe **13**, 66–69 (2005).
[49]J. Desarnaud, F. Bertrand, and N. Shahidzadeh–Bonn, "Dynamics of salt crystallization," in *Proceedings of SWBSS*, edited by I. Ioannou and M. Theodoridou (2011), p. 23.
[50]B. Lubelli, R. P. J. van Hees, H. P. Huinink, and C. J. W. P. Groot, Cem. Concr. Res. **36**, 678 (2006).